frontiers | Frontiers in Pharmacology

TYPE Original Research
PUBLISHED 08 August 2025
DOI 10.3389/fphar.2025.1575106

OPEN ACCESS

EDITED BY
Maria Dimitrova,
Medical University Sofia, Bulgaria

REVIEWED BY
Hua Li,
Air Force Medical University, China
Jingjing Liu,
Yangzhou University, China

*CORRESPONDENCE
Yaxing Zhang,
zhangyaxing@gzucm.edu.cn
Haimei Liu,
lhmei99@gzucm.edu.cn
Fuman Yan,
yanfuman@gzucm.edu.cn

†These authors have contributed equally to this work

‡Lead Contact

RECEIVED 11 February 2025
ACCEPTED 04 July 2025
PUBLISHED 08 August 2025

CITATION
Chen Y, Wang K, Guo W, Lu C, Suo W, Li Q, Deng Y, Chen X, Dai M, Zhang X, Xu J, Su W, Yang S, Yang H, Yan F, Liu H and Zhang Y (2025) Hydrogen gas (H_2) delivered by intraperitoneal injection alleviated methionine- and choline-deficient diet-induced metabolic dysfunction–associated steatotic liver disease in mice via inhibiting GSDMD- and GSDME-mediated pyroptosis.
Front. Pharmacol. 16:1575106.
doi: 10.3389/fphar.2025.1575106

Hydrogen gas (H_2) delivered by intraperitoneal injection alleviated methionine- and choline-deficient diet-induced metabolic dysfunction–associated steatotic liver disease in mice via inhibiting GSDMD- and GSDME-mediated pyroptosis

Yun Chen[1,2†], Kangrong Wang[1,2†], Wenhai Guo[3†], Chengqin Lu[1,2], Wenting Suo[1,2], Qiuling Li[1,2], Yao Deng[1,2], Xinling Chen[1,2], Min Dai[3,4,5], Xiaodong Zhang[1], Jiean Xu[1,2], Wen Su[1], Shuangling Yang[6], Hongzhi Yang[3], Fuman Yan[1]*, Haimei Liu[1,2]* and Yaxing Zhang[1,2*‡]

[1]Department of Physiology, School of Basic Medical Sciences, Guangzhou University of Chinese Medicine, Guangzhou, Guangdong, China, [2]Research Centre of Basic Integrative Medicine, School of Basic Medical Sciences, Guangzhou University of Chinese Medicine, Guangzhou, Guangdong, China, [3]Department of Traditional Chinese Medicine, The Third Affiliated Hospital, Sun Yat-sen University, Guangzhou, Guangdong, China, [4]Institute of Integrated Traditional Chinese and Western Medicine, Sun Yat-sen University, Guangzhou, Guangdong, China, [5]Department of Allergy and Immunology, The Third Affiliated Hospital, Sun Yat-sen University, Guangzhou, Guangdong, China, [6]School of Health Sciences, Guangzhou Xinhua University, Guangzhou, Guangdong, China

Background: Hydrogen gas (H_2), which is the lightest and diffusible gas molecule, has strong abilities to alleviate excessive oxidative stress, inflammation, and apoptosis. Inhalation of H_2 is beneficial for preventing the damage of the lung, heart, brain, liver, kidneys, and many other organs. However, the effect of intraperitoneal injection of H_2 on metabolic dysfunction–associated steatotic liver disease (MASLD) is unclear.

Objective: The aim of this study is to investigate whether intraperitoneal injection of H_2 can improve MASLD, and if so, what are the key innate immune mechanisms involved?

Methods: The MASLD mouse model was established by feeding a methionine- and choline-deficient (MCD) diet for 3 weeks. H_2 was daily given by intraperitoneal injection since the eighth day of MCD diet feeding, and lasted for 2 weeks. Serum levels of alanine aminotransferase (ALT) and aspartate aminotransferase (AST) were examined to evaluate liver injury. Hematoxylin and eosin (H&E) staining, Oil Red O staining, qPCR analysis of hepatic lipid metabolism genes, and detection of hepatic triglyceride (TG) levels were performed to evaluate hepatic steatosis. Masson trichrome staining and Collagen-I and Collagen-III protein levels were used to

evaluate liver fibrosis. The liver 3-nitrotyrosine (3-NT) was detected by immunoblotting and immunofluorescence, and the levels of malondialdehyde (MDA) and reduced glutathione (GSH) were measured using kits to evaluate redox homeostasis. The activation of TLR4-mediated innate immune signaling and pyroptosis were tested by immunoblotting and immunofluorescence. Moreover, hepatic protective effect and anti-pyroptosis effect of H_2 were further confirmed by H_2-rich DMEM-treated HepG2 cells *in vitro*.

Results: Supplementing with H_2 by intraperitoneal injection protected MCD diet-fed mice against hepatic steatosis and fibrosis by down-regulating *de novo* lipogenesis and fatty acid uptake genes, as well as hepatic Collagen-I and Collagen-III protein levels, while up-regulating lipid export genes. Mechanistically, H_2 modulated hepatic redox homeostasis by suppressing 3-NT and MDA levels, while increasing the reduced GSH levels. Subsequently, reactive oxygen species (ROS)-related innate immune signaling, including the expression of TLR4, and the activation of NF-κB, ERK1/2, p38 MAPK, and JNK in the liver, were all inhibited by H_2 treatment. These further contributed to inhibiting the expression of TNF-α, IL-1β, and IL-18 in the liver. The maturation of IL-1β and IL-18, the full-length of the classical pyroptosis trigger GSDMD, and the cleavage of GSDMD processed by Caspase-1 in NLRP3 inflammasome (including NLRP3, ASC, Caspase-1) were all blocked by H_2. In addition, H_2 decreased both the full-length and cleaved forms of Caspase-11, Caspase-8, Caspase-3 and GSDME, and thus inhibiting the non-canonical pyroptosis signaling in the liver of MASLD mice. The anti-pyroptosis effects of H_2 *in vitro* were further confirmed by the reduced expression of inflammatory cytokines, the decreased full-length and cleaved forms of GSDMD and GSDME, and the reduced number of HepG2 cells with pyroptotic morphology.

Conclusion: H_2 is an anti-pyroptosis gas molecule, intraperitoneal injection of H_2 is a novel therapeutic strategy for MASLD that deserves further investigation.

KEYWORDS

intraperitoneal injection, MCD, TLR4, NLRP3, GSDMD, GSDME, pyroptosis

1 Introduction

Metabolic dysfunction–associated steatotic liver disease (MASLD, formerly known as non-alcoholic fatty liver disease (NAFLD)) is a dynamic chronic non-communicable liver disease, which displays hepatic steatosis with one or more cardiometabolic risk factors in the absence of other causes of hepatic steatosis, such as drug-induced or alcohol-related steatosis (Sarkar and Kushner, 2025). MASLD includes a broad spectrum of progressive steatotic liver conditions, ranging from isolated hepatic steatosis to metabolic dysfunction-associated steatohepatitis (MASH) with varying amounts of liver fibrosis, and 10%–20% of the patients still progress to cirrhosis and its complications—hepatocellular carcinoma (HCC) and end-stage liver disease (Chen et al., 2021; Mallet et al., 2024; Miao et al., 2024). The global prevalence of MASLD was estimated to be 30.2% (Amini-Salehi et al., 2024). Resmetirom, a liver-selective and thyroid hormone receptor B (THRB, the predominant thyroid hormone receptor isoform in the liver)-selective thyromimetic, is the only one and first FDA-approved drug for MASH (Sinha et al., 2024). Therefore, it is still urgent to find other effective therapeutic drugs for MASLD.

Oxidative stress, inflammation, insulin resistance, and cell death are implicated in the pathogenesis of MASLD (Zhang et al., 2020c). Hydrogen gas (H_2), the lightest gas molecule in nature, has antioxidant, anti-inflammatory, and anti-apoptotic effects (Tan et al., 2019). Inhalation of H_2, drinking H_2-rich water and intraperitoneal injection of H_2-rich saline can alleviate many liver diseases, such as ischemia/reperfusion (I/R) injury and MASLD (Sun et al., 2011; Zhai et al., 2017; Ge et al., 2019; Liang et al., 2023; Liu et al., 2023). Our group and others have shown that intraperitoneal injection of H_2 can alleviate acute alcoholic liver injury and lipopolysaccharide (LPS)-induced cardiac dysfunction in mice (Tan et al., 2019; Zhang et al., 2021a; Xu et al., 2024), and display the neuroprotection in rabbits with cardiac arrest (Huang et al., 2013). However, the therapeutic effect of intraperitoneal injection of H_2 on MASLD are unknown, if it has a liver protective effect, what is the key mechanism?

2 Materials and methods

2.1 H_2 and H_2-rich medium

H_2 used for animals was daily prepared by injecting H_2 (Cat#73405157, Dalian Special Gases Co., Ltd., Dalian, China; >99.999%) into a 100 mL vacuumed infusion bottle (Guangdong Kelun Pharmaceutical Co., Ltd., Meizhou, China). H_2-rich Dulbecco's modified Eagle's medium (DMEM) for cell culture was prepared as we previously described. All these were shown in Figures 1A,B.

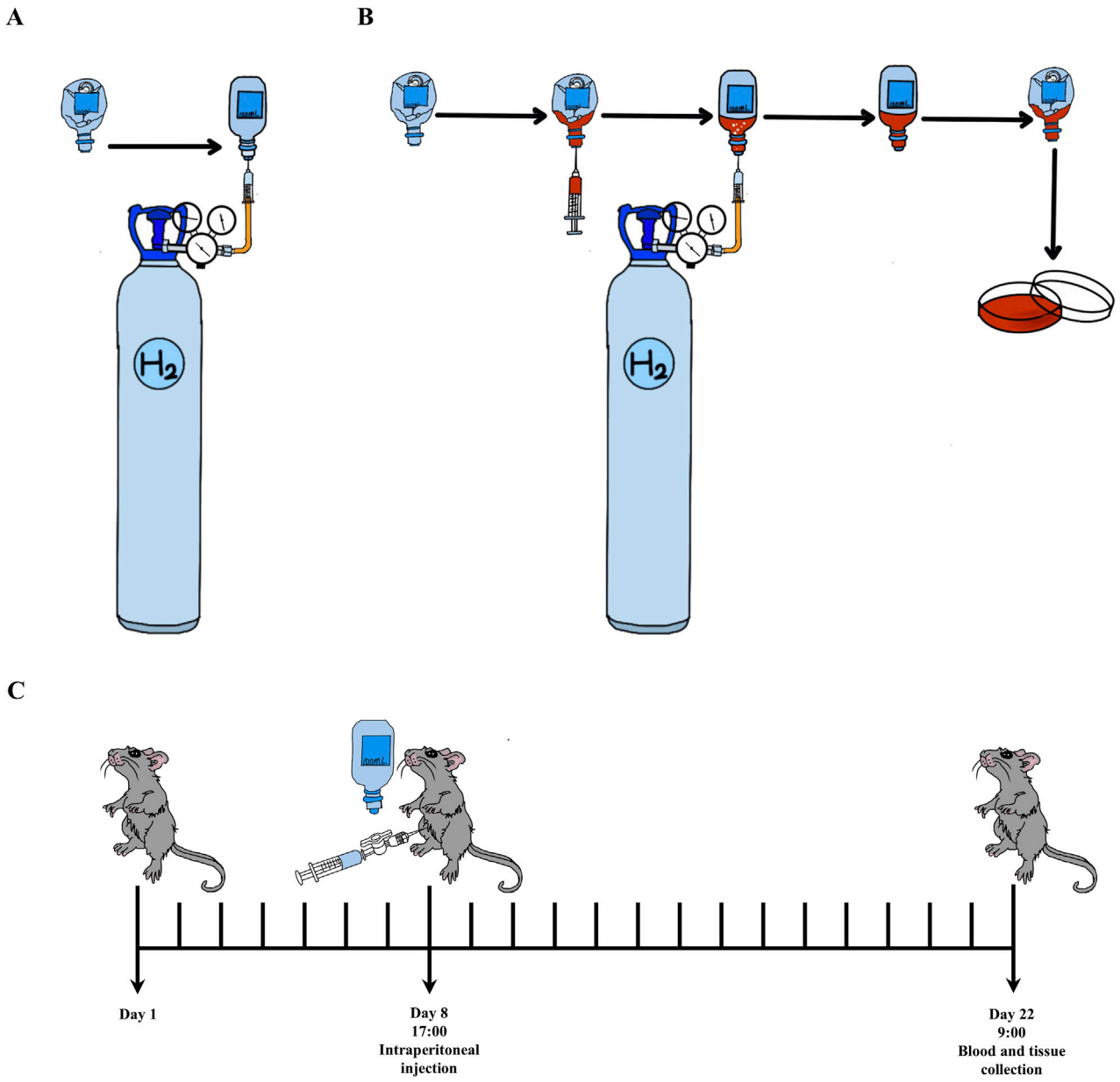

FIGURE 1
The methods of H_2 usage and experimental process. **(A)** Open the pressure reducing valve with a small release pressure, exhaust the air in the plastic hose connected to the pressure reducing valve. Insert the syringe needle into the evacuated plastic infusion bottle (100 mL), then further loosen the pressure reducing valve and introduce H_2 into the infusion bottle until there is no dead volume. **(B)** H_2-rich medium was prepared by introducing H_2 into the infusion bottle containing 10 mL DMEM until there is no dead volume, then, it was stored in 4°C for 6 h before used. **(C)** The experimental procedure is as follows: animals in H_2 treatment group are intraperitoneally injected with H_2 once a day at 5:00 p.m. since the eighth day. On day 22nd at 9:00 a.m., blood and liver samples are collected. In detail, there is a two-way valve connected between the injector and needle for injecting H_2. Open the two-way valve, extract the required volume of H_2 into the syringe, and immediately close the two-way valve. After removing the needle from the infusion bottle, immediately insert the needle into the abdominal cavity of the animals, open the two-way valve to complete the intraperitoneal injection.

2.2 Animal model of metabolic dysfunction-associated steatotic liver disease and H_2 treatment

The male C57BL/6 mice were brought from Guangdong Medical Laboratory Animal Center (Foshan, China). They were housed in an SPF animal facility with a 12-h light/dark cycle and *ad libitum* access to diet and water. All experimental procedures of animals were approved by the Institutional Animal Care and Use Committee (IACUC) of Guangzhou University of Chinese Medicine as a sub project of the "Building a Comprehensive Prevention and Treatment System for Cardiometabolic Diseases (3-1)" (Approval No. 2023053006).

The MASLD mouse model was established by feeding a MCD diet for 3 weeks (Henao-Mejia et al., 2012; Valdecantos et al., 2017; Figure 1C). Two doses of H_2 were used in this study (Xu et al., 2024). C57BL/6 mice (26–28 g) were randomly divided into four groups, including Control group, MCD group, MCD + H_2 (Low, L) group, and MCD + H_2 (High, H) group. The animals in the corresponding

group were fed a mixed diet for 3 days, as 50% standard chow plus 50% MCD Control diet (Cat#MD12051, Medicience Ltd., Yangzhou, China) for Control group, and 50% standard chow plus 50% MCD diet (Cat#MD12052, Medicience Ltd., Yangzhou, China) for the other three groups, and subsequently, mice in the corresponding group were fed a MCD Control diet or a MCD diet for another 18 days. On day eighth, mice were daily given H_2 by intraperitoneal injection at the doses of 0.5 mL/100 g for MCD + H_2 (L) group, and 1.0 mL/100 g for MCD + H_2 (H) group. On day 22nd, mice were deeply anesthetized before blood collection from the orbital sinus, and then, euthanized via cervical dislocation (Mackowiak et al., 2022). The liver samples were frozen in −80°C or put in 4% Paraformaldehyde Fix Solution (Cat#G1101, Servicebio, Wuhan, China) for further analysis.

2.3 Sodium oleate-induced lipid accumulation in HepG2 cells and treatment by H_2-rich medium

HepG2 cells, which were generously provided by Prof. Peng Zhang (School of Basic Medical Sciences, Wuhan University, China), were cultured in DMEM containing 10% fetal bovine serum (FBS) and 1% penicillin-streptomycin in a cell culture incubator with 5% CO_2 at 37°C. Oleic acid (OA)-induced lipid accumulation HepG2 cell model was established by sodium oleate (Cat#S6130, Solarbio, Beijing, China) (Chen et al., 2020; Liu et al., 2020; Wang et al., 2022). HepG2 cells were divided into four groups: Control group, OA group, OA+H_2 group, and H_2 group. H_2-rich DMEM with 1% FBS was added to the OA+H_2 and H_2 groups, and the Control group and OA group were treated with the same volume of H_2-free DMEM with 1% FBS. HepG2 cells in the OA group and OA+H_2 group were treated with sodium oleate (0.25 mM) for 18 h after 30 min of H_2 treatment.

2.4 Serum ALT and AST, and hepatic MDA, reduced GSH and TG analysis

Serum levels of alanine aminotransferase (ALT) and aspartate aminotransferase (AST) were examined by an automatic blood chemistry analyzer in Department of Clinical Laboratory from The Third Affiliated Hospital of Sun Yat-sen University (Xu et al., 2024). Hepatic malondialdehyde (MDA), reduced glutathione (GSH), and triglycerides (TG) levels were examined by the commercialized reagent kits (Cat#A003-1-2, A006-2-1, and A110-1-1, Nanjing Jiancheng Bioengineering Institute, Nanjing, China).

2.5 Histopathological analysis

The fixed liver tissues by 4% paraformaldehyde fixed solution for over 24 h were embedded in paraffin and sliced into 4 μm sections. Then, Masson's trichrome (Cat#G1006-100ML, Servicebio, Wuhan, China) staining, and Hematoxylin (Cat#BA4097-500ML, BaSo, Zhuhai, China) and eosin (Cat#BA4099-500ML, BaSo, Zhuhai, China) (H&E) staining was performed according to the standard procedures. In H&E-stained pathological sections, hepatic steatosis was scored and the severity was graded based on the percentage of affected total area, into the following categories: 0 (<5%), 1 (5%–33%), 2 (>33–66%), and 3 (>66%) (Kleiner et al., 2005; Liang et al., 2014; Zhang et al., 2020c). The H&E image analysis was performed by Chengqin Lu and Yun Chen, and a double-blind design was implemented to minimize bias. HepG2 cells were fixed with 4% paraformaldehyde, and the frozen liver sections (10 μm) were prepared in Tissue-Tek® optimum cutting temperature (O.C.T.) compound (Cat#4583, Sakura, Japan), then, they stained with Oil Red O (Cat#G1015-100ML, Servicebio, Wuhan, China). Hepatic lipid accumulation by Oil Red O staining in the liver tissues were quantified as previously described (Mehlem et al., 2013).

2.6 Quantitative PCR (qPCR) analysis

Total RNA was extracted from the fresh liver tissues by EZ-press RNA Purification Kit (Cat#B0004DP, EZBiocience, Roseville, CA, United States), Color Reverse Transcription Kit (Cat#A0010CGQ, EZBiocience, Roseville, CA, United States) was used to convert mRNA to cDNA, and 2 * Color SYBR Green qPCR Master Mix (Cat#A0012-R2, EZBiocience, Roseville, CA, United States) was used for qPCR under the standard procedure. The target genes levels were normalized to glyceraldehyde-3-phosphate dehydrogenase (*Gapdh*) by $2^{-\triangle\triangle ct}$. The primer sequences of target genes were described in Table 1.

2.7 Western blot

Total proteins in the liver samples were extracted by the lysis buffer containing 4% protease inhibitor cocktail (Cat#4693132001, Roche, 25×) and 10% phosphatase inhibitor cocktail (Cat#4906837001, Roche, 10×) (Zhang et al., 2020b). The expression levels of the corresponding proteins in the liver samples were determined by Western blot according to the standard processes (Zhang et al., 2021a). The antibodies used in this study were listed in Table 2.

2.8 Immunofluorescence staining

3-NT immunofluorescence staining was performed on frozen sections of the liver samples as follows: (1) Wash frozen sections with PBS for 30 min, with TBS for 10 min, and with TBST for 20 min (2) Seal with goat serum blocking solution (Cat#ZLI-9056, ZSGB Bio, Beijing, China) at room temperature for 2 h (3) Incubate overnight with 3-NT antibody (see Table 1) at 4°C. (4) Wash with TBS for 10 min, with TBST for 20 min (5) Incubate with Goat Anti-Mouse IgG (H+L) Fluor 594-conjugated secondary antibody (Cat#S0005, Affinity Biosciences, Beijing, China) under dark conditions for 2 h (6) Wash with TBS for 10 min, with TBST for 20 min (7) Finally, the fluorescence intensity of 3-NT was observed under a fluorescence microscope after sealing the sections with Mounting Medium, antifading (with DAPI) (Cat#S2110, Solarbio, Beijing, China).

2.9 Statistical analysis

The statistical analyses were performed by one-way analysis of variance (ANOVA) followed by Bonferroni's *post hoc* analysis for data

TABLE 1 Sequences of primers used for real-time quantitative PCR.

Gene	Forward primer sequence (5′–3′)	Reverse primer sequence (5′–3′)
Gapdh	AGAACATCATCCCTGCATCC	TTGTCATTGAGAGCAATGCC
Fasn	GCCATGCCCAGAGGGTGGTT	AGGGTCGACCTGGTCCTCA
Acaca	TGGAGCTAAACCAGCACTCC	GCCAAACCATCCTGTAAGCC
Cpt1a	ATCGTGGTGGTGGGTGTGATAT	ACGCCACTCACGATGTTCTTC
Acox	TGTCATTCCTACCAACTGTC	CCATCTTCTCAACTAACACTC
CD36	GTGCAAAACCCAGATGACGT	TCCAACAGACAGTGAAGGCT
Fabp1	GCAGAGCCAGGAGAACTTTGAG	TTTGATTTTCTTCCCTTCATGCA
Mttp	AACTCCTACGAGCCCTCCTT	AGTCCTCCCAGGATCAGCTT
Apob	TCACCATTTGCCCTCAACCTAA	GAAGGCTCTTTGGAAGTGTAAAC
Ppara	AGAGCCCCATCTGTCCTCTC	ACTGGTAGTCTGCAAAACCAAA

TABLE 2 The antibodies.

Antibodies	Catalog numbers	Suppliers
Anti-rabbit IgG HRP-linked antibody	#S0001	Affinity Biosciences
Anti-mouse IgG HRP-linked antibody	#S0002	Affinity Biosciences
TNF-α antibody	#AF7014	Affinity Biosciences
Collagen I Antibody	#AF7001	Affinity Biosciences
Collagen III Antibody	#AF0136	Affinity Biosciences
ASC	#DF6304	Affinity Biosciences
TLR4 antibody	#sc-293072	Santa Cruz Biotechnology
Caspase-3 antibody	#sc56053	Santa Cruz Biotechnology
Caspase-11 antibody	#sc-374615	Santa Cruz Biotechnology
Caspase-8 antibody	#9746S	Cell Signaling Technology
p-NF-κB p65 antibody	#3033S	Cell Signaling Technology
NF-κB p65 antibody	#8242S	Cell Signaling Technology
NLRP3	#15101S	Cell Signaling Technology
Phospho-SAPK/JNK antibody	#9255S	Cell Signaling Technology
SAPK/JNK Antibody	#9252S	Cell Signaling Technology
p38 antibody	#8690S	Cell Signaling Technology
p-p38 antibody	#4511S	Cell Signaling Technology
MAPK (Erk1/2) antibody	#4695S	Cell Signaling Technology
Rabbit Anti-phospho-ERK1/2 (Thr202 + Tyr204) antibody	bs-3016R	Bioss
IL-18 antibody	#D046-3	Medical and Biological Laboratories Co., Ltd.
GAPDH antibody	#MB001	Bioworld Technology
3-nitrotyrosine (3-NT) antibody	#ab110282	Abcam
GSDMD antibody	#ab219800	Abcam
GSDME antibody	#ab215191	Abcam
Caspase-1 antibody	#ab1872	Abcam

10.3389/fphar.2025.1575106

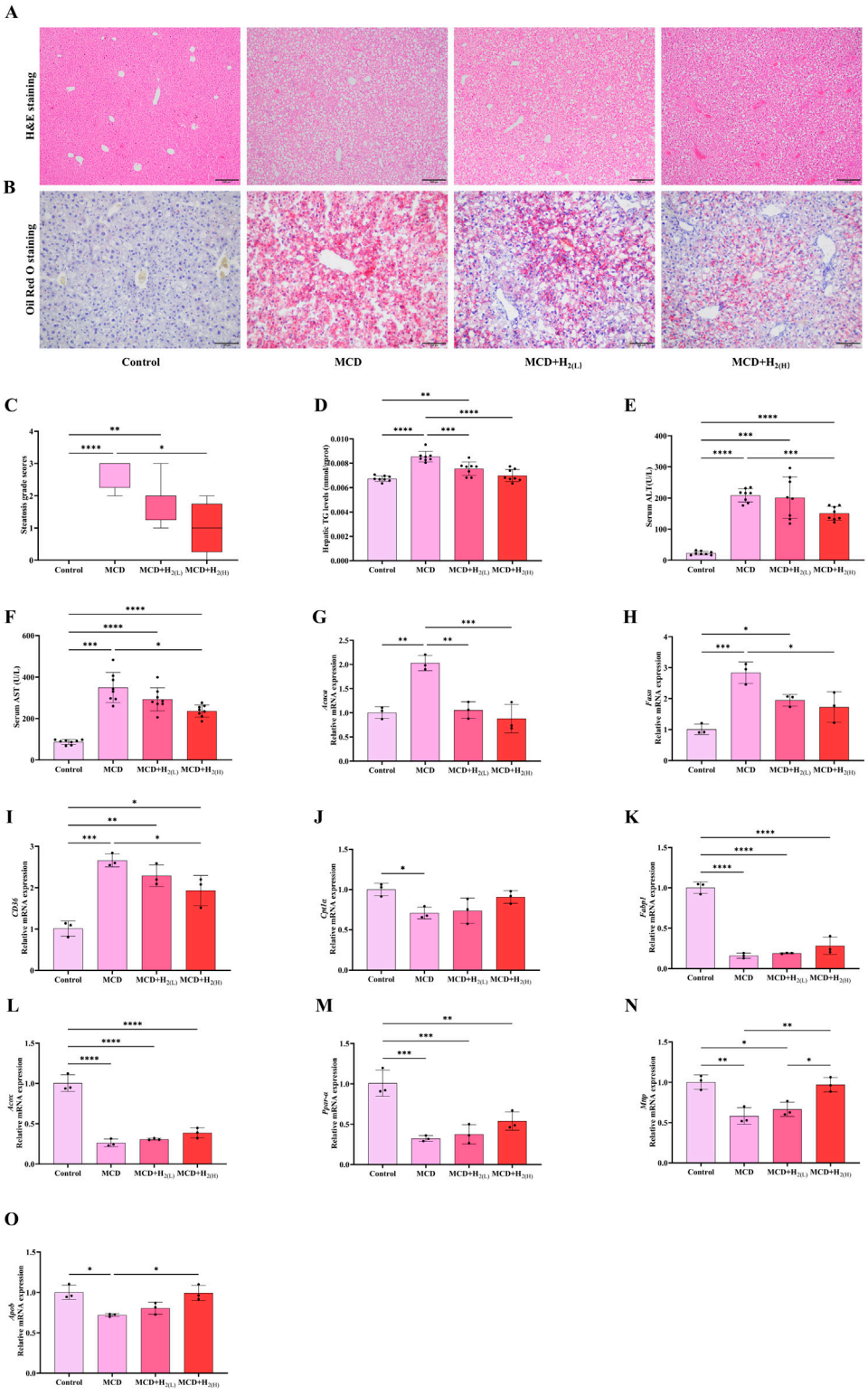

FIGURE 2
H_2 therapy improved hepatic steatosis in mice fed with a MCD diet. **(A)** Liver H&E and **(B)** Oil Red O staining showed that both low and high doses of H_2 attenuated MCD-induced hepatic steatosis. **(C)** Steatosis grade score, n = 8 mice in each group. **(D)** The levels of TG in the liver tissues, **(E)** Serum ALT levels, **(F)** Serum AST levels, n = 8 mice in each group. **(G)** The relative mRNA levels (ratios to *Gapdh*) of *Acaca*, **(H)** *Fasn*, **(I)** *CD36*, **(J)** *Cpt1α*, **(K)** *Fabp1*, **(L)** *Acox*, **(M)** *Ppar-α*, **(N)** *Mttp*, **(O)** *Apob*, n = 3 mice in each group. The data of steatosis grade score are expressed as median ± interquartile range, other results are expressed as means ± SD. *p < 0.05, **p < 0.01, ***p < 0.001, ****p < 0.0001.

with normal distribution (by Shapiro-Wilk test) and satisfying homogeneity of variance (by Brown-Forsythe test), performed by Brown-Forsythe and Welch ANOVA tests followed by Dunnett T3 *post hoc* analysis for data with normal distribution and heteroscedasticity, and performed by Kruskal-Wallis test followed by Dunn's *post hoc* analysis for data with skewed distributions (by Shapiro-Wilk test). All data were expressed as mean ± SD or median ± interquartile range, a value of $P < 0.05$ was considered as significantly different. All histograms were performed using GraphPad Prism 10.1.2 (GraphPad Software Inc., San Diego, CA, United States).

3 Results

3.1 H_2 improved hepatic steatosis in mice fed with a MCD diet

The basic characteristics of MASLD is hepatic steatosis (Rinella et al., 2023; Hagström et al., 2024). Therefore, we first investigated that whether supplementing with H_2 through intraperitoneal injection has a protective effect on lipid deposition in the liver of mice fed with a MCD diet. Macrovesicular steatosis indicated by H&E staining (Figure 2A) and lipid droplets indicated by Oil red O staining (Figure 2B) were obviously visible in MCD group. The steatosis grade scores (Figure 2C), and hepatic TG levels (Figure 2D) were higher in MCD group than Control group. The increased serum levels of ALT (Figure 2E) and AST (Figure 2F) pointed to hepatocellular injury in MCD group. All these indicators reflecting hepatic steatosis and liver injury were improved by high dose H_2 therapy. Hepatic steatosis is a consequence of lipid acquisition exceeding lipid disposal, for example, fatty acid uptake and *de novo* lipogenesis surpassing lipid export and fatty acid oxidation (Ipsen et al., 2018). Here, we found the hepatic mRNA involved in *de novo* lipogenesis, such as acetyl-Coenzyme A carboxylase (*Acaca*) and fatty acid synthetase (*Fasn*), and fatty acid uptake gene *CD36* were increased by feeding a MCD diet for 3 weeks (Figures 2G-I); in contrast, the genes involved in fatty acid oxidation, such as carnitine palmitoyl transferase 1 α (*Cpt1α*) and fatty acid binding protein 1 (*Fabp1*), Acyl-CoA oxidase (*Acox*, the rate-limiting enzyme in peroxisomal β-oxidation of fatty acids), and peroxisome proliferator-activated receptor-α (*PPAR-α*) (Figures 2J-M), the lipid exporting genes such as microparticle triglyceride transfer protein (*Mttp*) and apolipoprotein B (*Apob*) were decreased by feeding a MCD diet for 3 weeks (Figures 2N,O). Among these, *Acaca*, *Fasn*, and *CD36* were decreased (Figures 2G-I), while *Mttp* and *Apob* were increased by high dose H_2 therapy (Figures 2N,O). Therefore, these data indicated that H_2 can improve hepatic steatosis in mice fed with a MCD diet probably via inhibiting *de novo* lipogenesis and fatty acid uptake, while increasing lipid export.

3.2 H_2 improved liver fibrosis in mice fed with a MCD diet

MASLD patients have the potential for progressively developing into liver fibrosis (Chalasani et al., 2017; Younossi et al., 2023). Our Masson staining indicated that MCD diet feeding induced liver fibrosis in mice, and the hepatic protein levels of fibrosis markers Collagen-I and Collagen-III, were increased in mice fed with a MCD diet, these conditions were all improved by H_2 therapy (Figure 3). Therefore, these data indicated that H_2 also has the potential to improve liver fibrosis in mice fed with a MCD diet.

3.3 H_2 alleviated oxidative stress in the liver of mice fed with a MCD diet

Hepatic oxidative stress is a key feature and contributor of MASLD (Li et al., 2024). To investigate the effects of intraperitoneal injection of H_2 on oxidative damage in the liver of mice fed with a MCD diet, hepatic 3-nitrotyrosine (3-NT), an indicator of oxidative stress, were examined by immunofluorescence and Western blot. Compared with Control group, 3-NT levels in the liver were elevated in MCD group, and it was decreased by H_2 therapy (Figures 4A–D). Malondialdehyde (MDA) is an aldehyde formed as secondary products during lipid peroxidation, in contrast, glutathione (GSH) is a principal intracellular antioxidant buffer (Ayala et al., 2014; Wrotek et al., 2020). We further evaluated MDA and GSH levels in the liver. Hepatic MDA levels were increased, while hepatic reduced GSH levels were decreased in MCD group when compared with Control group, in contrast, H_2 therapy reversed this redox imbalance (Figures 4E,F). Therefore, H_2 therapy alleviated oxidative stress in the liver of mice fed with a MCD diet.

3.4 H_2 suppressed pyroptosis in the liver of mice fed with a MCD diet

In human and murine models of MASH, increased hepatocyte death, such as apoptosis and pyroptosis, is a critical mechanism contributing to inflammation and fibrogenesis (Hatting et al., 2013; Xu et al., 2018; Gaul et al., 2021). The canonical proptosis, a lytic form of cell death, can be elicited by Caspase-1 (which is activated after the binding of the ligands to the inflammasome-forming pattern recognition receptors (PRRs), such as NLRP3 (Shi et al., 2015)) to cleave the pyroptosis executioner, gasdermin D (GSDMD) (Shi et al., 2017). The gasdermin-N domains of GSDMD can bind the membrane lipids, phosphoinositides and cardiolipin, and exhibit membrane-disrupting cytotoxicity in mammalian cells, and thus triggering pyroptosis (Ding et al., 2016). In order to investigate the effect of H_2 on NLRP3 inflammasome activation and the subsequent pyroptosis in the liver of mice fed with a MCD diet, we examined NLRP3, ASC, Caspase-1 and GSDMD protein levels in the liver. Our results showed that MCD diet feeding increased the protein levels of NLRP3 and ASC, and the full length and cleaved forms of Caspase-1 and GSDMD in the liver, in contrast, these upregulation were decreased by H_2 therapy (Figure 5). In addition to Caspase-1-GSDMD pathway, the non-canonical pathway can also induce pyroptosis, as the cleavage of GSDMD by Caspaes-11/8 and the cleavage of GSDME specifically by Caspase-3 (Kayagaki et al., 2015; Wang et al., 2017; Sarhan et al., 2018). Here, we showed that compared with Control group, the full length and cleaved forms of Caspase-11, Caspase-8, Caspase-3, and GSDME were increased, while H_2 downregulated both the expression and maturation of these pyroptosis signaling proteins (Figure 6). Therefore, H_2 inhibited pyroptosis in the liver of mice fed with a MCD diet.

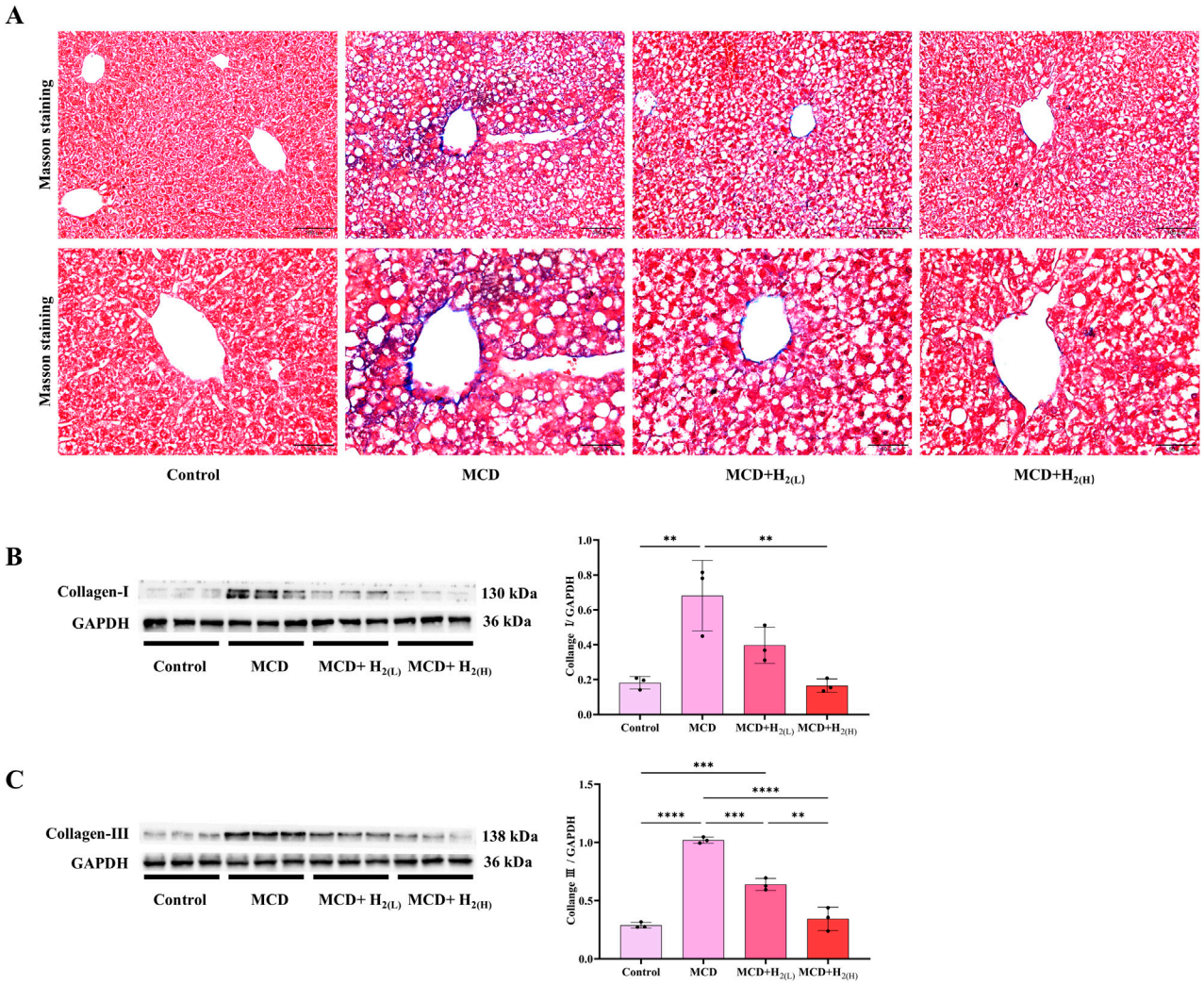

FIGURE 3
The effect of H_2 on liver fibrosis in mice fed with a MCD diet. **(A)** The Masson's trichrome staining showed that H_2 alleviated mild liver fibrosis induced by MCD. **(B)** Western blotting images of hepatic Collagen-I and GAPDH, and quantification of Collagen-I/GAPDH ratio, **(C)** Western blotting images of hepatic Collagen-III and GAPDH, and quantification of Collagen-III/GAPDH ratio, n = 3 mice in each group. Results are expressed as means ± SD. **p < 0.01, ***p < 0.001, ****p < 0.0001.

3.5 H_2 therapy reduced inflammatory cytokines expression in the liver of mice fed with a MCD diet

The activated Caspase-1 can process the cleavage of GSDMD and IL-1β, and the cleavage of GSDMD is required for pyroptosis and the release of matured IL-1β (He et al., 2015; Shi et al., 2015). It is well-known that the increased inflammatory cytokines were essential for the pathogenesis of MASLD. Therefore, we examined hepatic protein levels of inflammatory cytokines to explore the effects of intraperitoneal injection of H_2 on inflammation in mice with MASLD. Our results showed that compared with Control group, the hepatic levels of TNF-α, the full length and cleaved forms of IL-1β and IL-18 were all increased in MCD group, and high dose H_2 therapy reversed the upregulation of these inflammatory cytokines in the liver (Figure 7). Therefore, H_2 therapy inhibited inflammatory cytokines expression in the liver of mice fed with a MCD diet.

3.6 H_2 inhibited the overactivation of TLR4 innate immune signaling in the liver of mice fed with a MCD diet

The expression of hepatic inflammatory cytokines were induced by the activation of pattern recognition receptors (PRRs, such as Toll-like receptor 4 (TLR4)) after recognizing the upregulated pathogen-associated molecular patterns (PAMPs, such as LPS) or damage associated molecular patterns (DAMPs) during the progression of MASLD (Carpino et al., 2020). Here, the expression of TLR4, and the phosphorylation of its downstream signaling proteins, including nuclear factor-κB (NF-κB), ERK1/2,

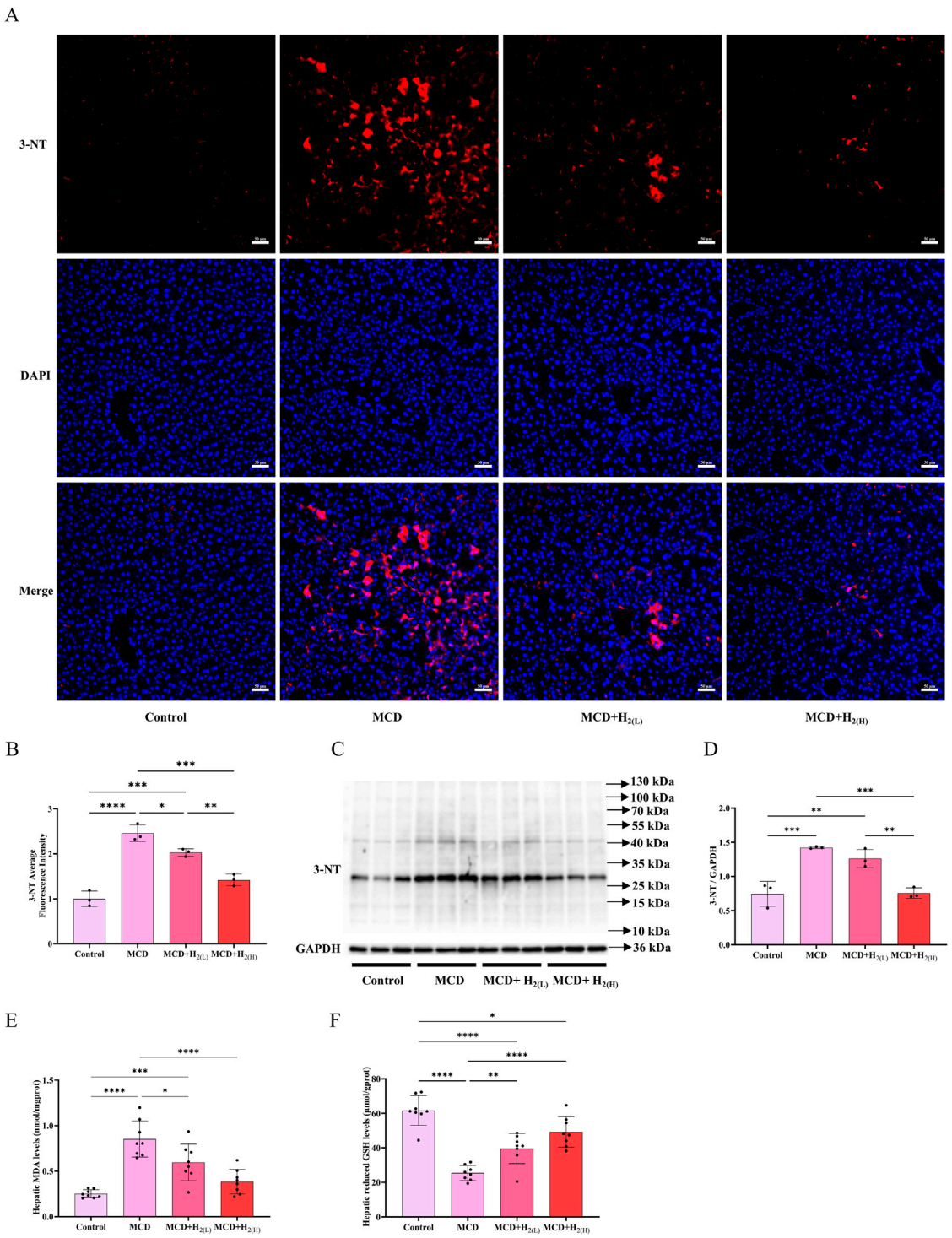

FIGURE 4
H_2 alleviated oxidative stress in the liver of mice fed with a MCD diet. **(A)** Immunofluorescence of 3-NT, **(B)** 3-NT average fluorescence intensity, **(C)** Western blotting images of hepatic 3-NT and GAPDH and **(D)** quantification of 3-NT/GAPDH ratio, n = 3 mice in each group. **(E)** Hepatic MDA and **(F)** the reduced GSH levels, n = 8 mice in each group. Results are expressed as means ± SD. *p < 0.05, **p < 0.01, ***p < 0.001, ****p < 0.0001.

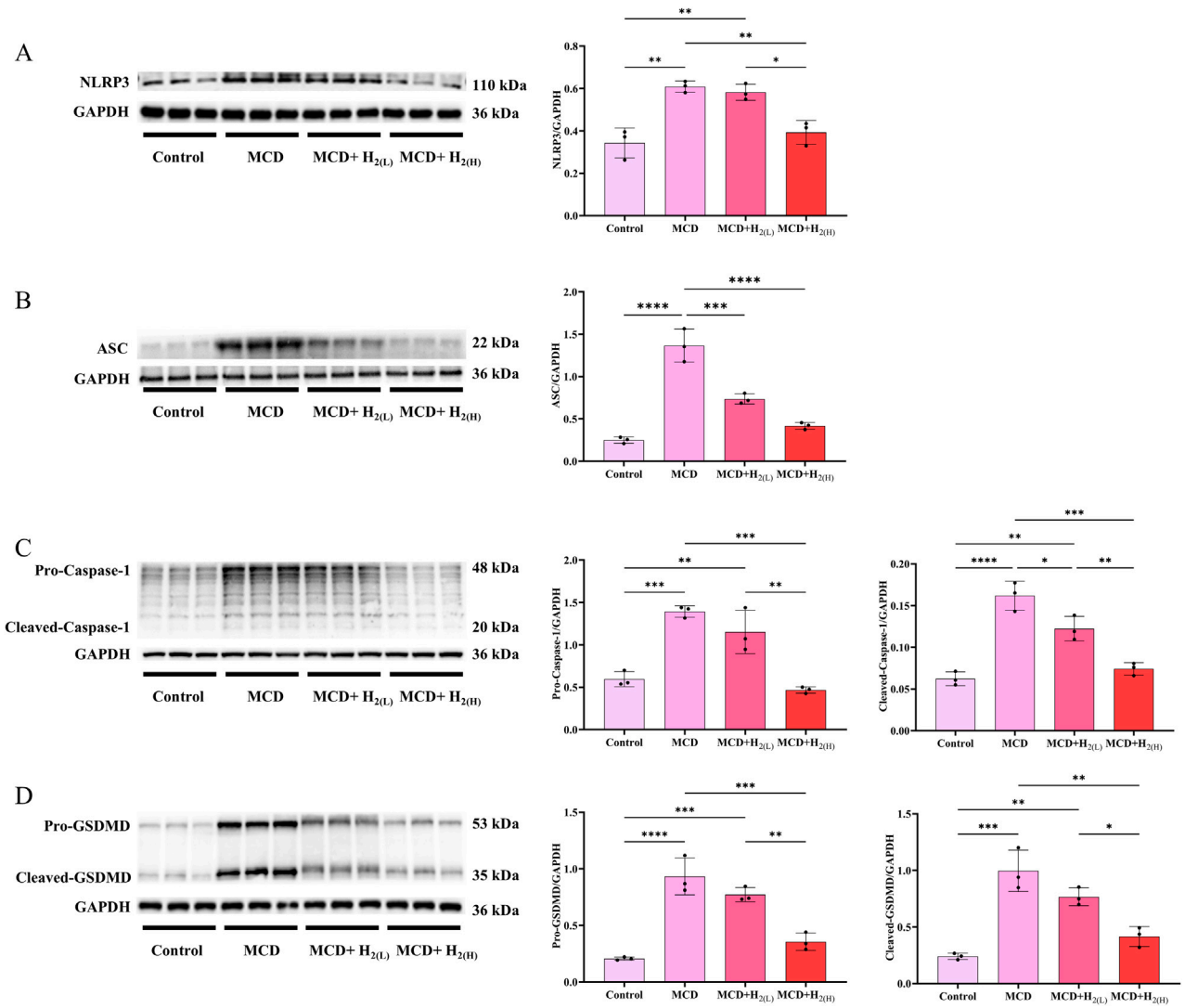

FIGURE 5
H_2 therapy inhibited hepatic NLRP3 inflammasome activation in mice fed with a MCD diet. **(A)** Western blotting images of hepatic NLRP3 and GAPDH, and quantification of NLRP3/GAPDH ratio; **(B)** Western blotting images of hepatic ASC and GAPDH, and quantification of ASC/GAPDH ratio; **(C)** Western blotting images of hepatic pro-Caspase-1, cleaved-Caspase-1 and GAPDH, and quantifications of pro-Caspase-1/GAPDH and cleaved-Caspase-1/GAPDH ratios; **(D)** Western blotting images of pro-GSDMD, cleaved-GSDMD and GAPDH in the liver, and quantifications of pro-GSDMD/GAPDH and cleaved-GSDMD/GAPDH ratios; n = 3 mice in each group. Results are expressed as means ± SD. *p < 0.05, **p < 0.01, ***p < 0.001, ****p < 0.0001.

p38 MAPK, and JNK, were all increased in the liver of mice fed with a MCD diet (Figure 8). In contrast, this overactivated TLR4 innate immune signaling was suppressed by intraperitoneal injection of high doses H_2 (Figure 8).

3.7 H_2-rich medium improved sodium oleate-induced HepG2 cells steatosis by inhibiting inflammatory cytokines expression and pyroptosis

The hepatic protection of H_2 on steatosis was further confirmed in sodium oleate (OA)-induced HepG2 cells steatosis model as indicated by Oil red O staining (Figure 9A). OA increased the expression of 3-NT (Figure 9B), TNFα (Figure 9C), IL1-β (Figure 9D) and IL-18 (Figure 9E) in HepG2 cells, these were all suppressed by H_2-rich medium. Moreover, OA increased the numbers of cells with the pyroptosis morphology as cell swelling with large bubbles (Figure 9F), increased the levels of full-length and cleaved forms of GSDMD (Figure 9G) and GSDME (Figure 9H), these indicated that OA elicited pyroptosis in HepG2 cells, which were all inhibited by H_2-rich medium treatment. Therefore, H_2-rich medium inhibited the expression of inflammatory cytokines, and targeted GSDMD and GSDME to alleviate OA-induced steatosis in HepG2 cells.

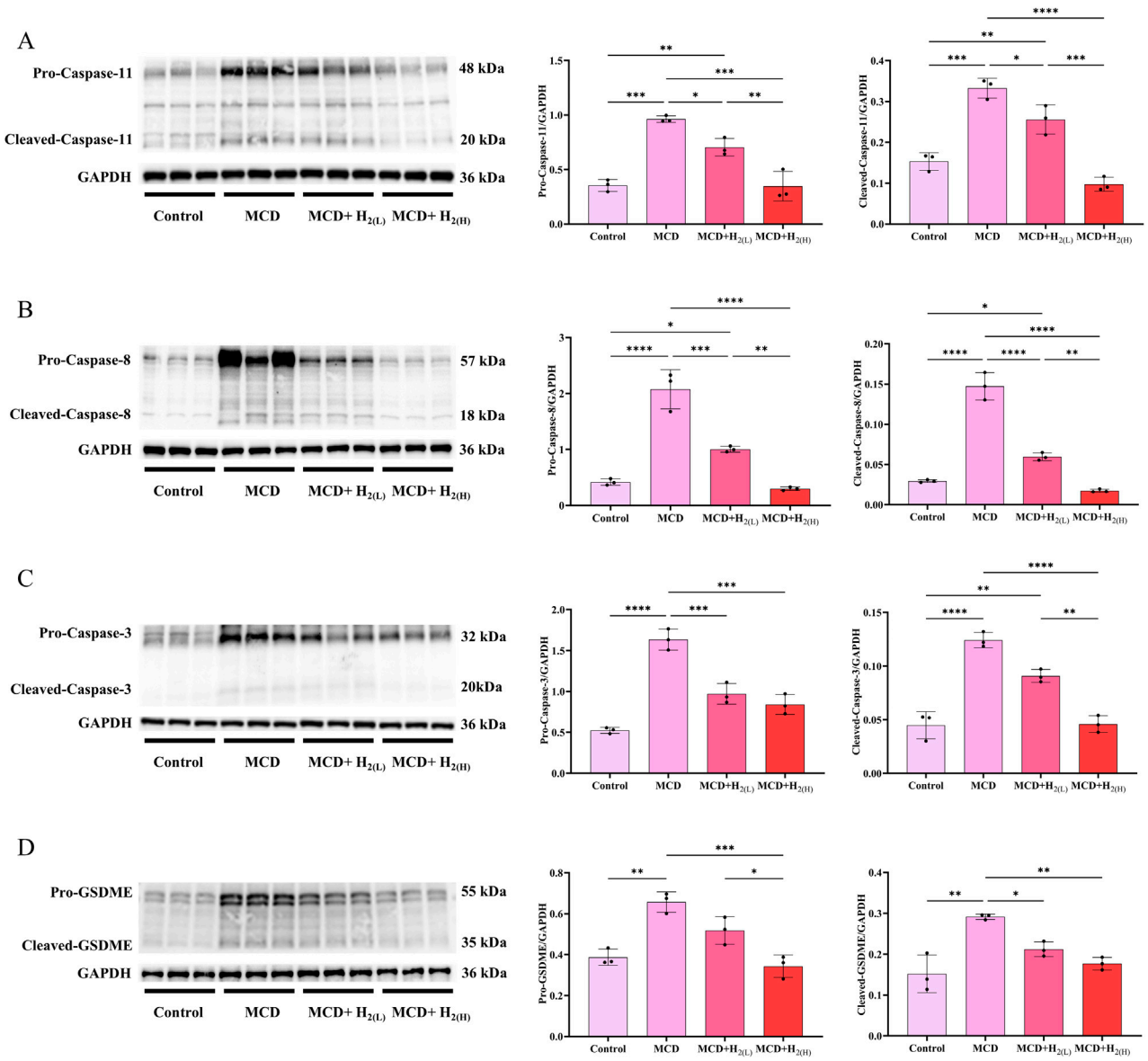

FIGURE 6
H_2 therapy inhibited the non-classical pyroptosis signaling in the liver of mice fed with a MCD diet. **(A)** Western blotting images of pro-Caspase-11, cleaved-Caspase-11 and GAPDH in the liver, and quantifications of pro-Caspase-11/GAPDH and cleaved-Caspase-11/GAPDH ratios; **(B)** Western blotting images of pro-Caspase-8, cleaved-Caspase-8 and GAPDH in the liver, and quantifications of pro-Caspase-8/GAPDH and cleaved-Caspase-8/GAPDH ratios; **(C)** Western blotting images of pro-Caspase-3, cleaved-Caspase-3 and GAPDH in the liver, and quantifications of pro-Caspase-3/GAPDH and cleaved-Caspase-3/GAPDH ratios; **(D)** Western blotting images of pro-GSDME, cleaved-GSDME and GAPDH in the liver, and quantifications of pro-GSDME/GAPDH and cleaved-GSDME/GAPDH ratios; n = 3 mice in each group. Results are expressed as means ± SD. *p < 0.05, **p < 0.01, ***p < 0.001, ****p < 0.0001.

4 Discussion

MASLD is the leading chronic liver disease worldwide. The spectrum of MASLD ranges from simple steatosis, through MASH, to fibrosis, and ultimately cirrhosis and HCC. Until March 2024, the US Food and Drug Administration (FDA) approved the launch of the first (and only) characteristic drug, resmetirom, for the treatment of fibrosis in MASH (Keam, 2024). Therefore, it is still urgent to find other effective treatments for MASH. H_2 is a gas molecule with anti-inflammation, anti-oxidation, and anti-apoptosis effects. Since Ikuroh Ohsawa first discovered that inhaling 2% H_2 can improve cerebral I/R injury in rats, the therapeutic effect of H_2 has attracted more attention (Ohsawa et al., 2007). So far, H_2 has been reported to have therapeutic effects in various liver diseases, such as alcoholic liver injury (Zhang et al., 2021a; Xu et al., 2024). Here, we first reported that intraperitoneal injection of H_2, as a novel strategy for supplementing exogenous H_2, can treat MCD diet-induced MASLD in mice. Future research should add a positive control group, using Resmetirom, to evaluate the efficacy of H_2.

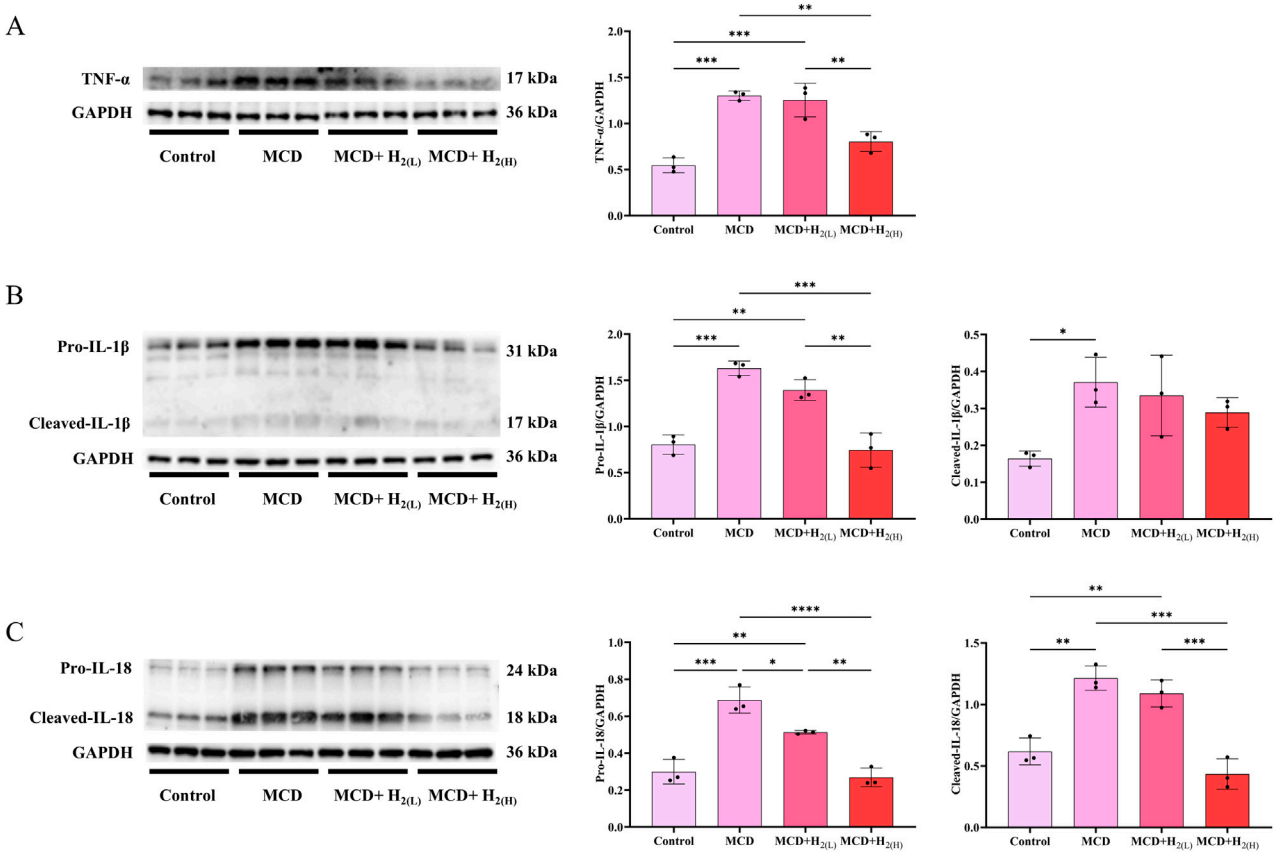

FIGURE 7
H_2 suppressed hepatic pro-inflammatory cytokines expression in mice fed with a MCD diet. **(A)** Western blotting images of TNF-α and GAPDH in the liver, and quantifications of TNF-α/GAPDH ratio, **(B)** Western blotting images of pro-IL-1β, cleaved- IL-1β and GAPDH in the liver, and quantifications of pro-IL-1β/GAPDH and cleaved- IL-1β/GAPDH ratios, **(C)** Western blotting images of pro-IL-18, cleaved- IL-18 and GAPDH in the liver, and quantifications of pro-IL-18/GAPDH and cleaved-IL-18/GAPDH ratios, n = 3 mice in each group. Results are expressed as means ± SD. *p < 0.05, **p < 0.01, ***p < 0.001, ****p < 0.0001.

Methionine or choline can stimulate the synthesis of phosphatidylcholine (the principal phospholipid comprising the outer coat of very-low-density lipoprotein (VLDL) particles), which is required for the secretion of VLDL and its deficiency induces lipid accumulation in the liver (Rizki et al., 2006). Our data showed that MCD diet feeding induced obvious hepatic steatosis in mice as indicated by H&E and oil red O staining, and the increased hepatic TG levels. MCD diet promotes hepatic lipid accumulation by more than one mechanism (Rinella et al., 2008). The four key events as *de novo* lipogenesis, fatty acid uptake, lipid export and fatty acid oxidation, are all involved in the pathogenesis of MASLD in animals induced by feeding a MCD diet, however, the degree of MASLD is related to the days of feeding, the differences in MCD dietary components, and the animal strains (Kirsch et al., 2003; Rizki et al., 2006; Gyamfi et al., 2008; Rinella et al., 2008; Pickens et al., 2009; Wu et al., 2010; Machado et al., 2015; Pierce et al., 2015; Xu et al., 2018; Yu et al., 2019). Here, we found that the genes involved in fatty acid uptake (*CD36*) and *de novo* lipogenesis (*Acaca* and *Fasn*) were increased and the genes involved in lipid export (*Mttp* and *Apob*) and fatty acid oxidation (Cpt1α, *Fabp1*, *Acox*, and *PPAR-α*) were decreased in the liver of male C57BL/6 mice fed with a MCD diet for 3 weeks. H_2 treatment decreased the mRNA levels of genes involved in *de novo* lipogenesis and fatty acid uptake, while increased the mRNA levels of genes involved in lipid export. In order to provide a precise answer on the effect of H_2 on hepatic lipid metabolism, we should further detect the protein levels and activities of these genes, and levels of related metabolites. H_2 also improve liver fibrosis and decreased hepatic Collagen-Ⅰ and Collagen-Ⅲ protein levels induced by MCD diet feeding. Therefore, H_2 has a therapeutic effect on MASLD in mice caused by feeding a MCD diet.

The pathophysiology underlying MASLD is complex and incompletely understood. In 1998, Day and James proposed two hits hypothesis, that the first hit is steatosis, and the second hit is oxidative stress (Day and James, 1998). In 2010, Tilg and Moschen further proposed multiple parallel hits hypothesis, many parallel hits, such as lipotoxicity, insulin resistance, oxidative stress, and the overactivation of both innate and adaptive immunity, contribute to the development of MASLD or MASH (Tilg and Moschen, 2010; Targher et al., 2024). Among these, oxidative stress is as a central mechanism driving MASLD, it results from an imbalance between the production and elimination of ROS (Hu et al., 2025). Here, oxidative stress indicators including 3-NT and

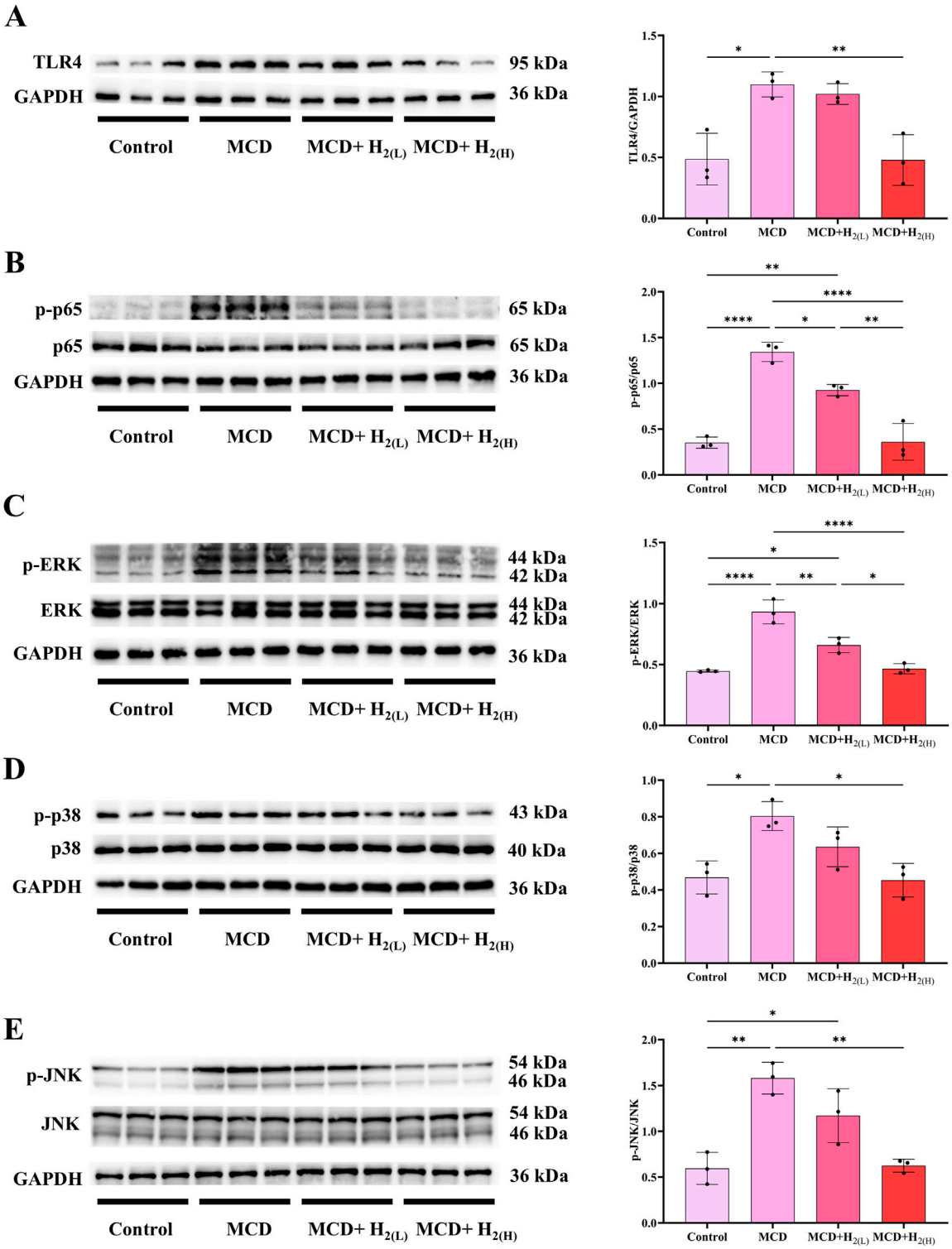

FIGURE 8
H_2 suppressed hepatic TLR4-NFκB and MAPK innate immune signaling in mice fed with a MCD diet. **(A)** Western blotting images of TLR4 and GAPDH in the liver, and quantifications of TLR4/GAPDH ratio; **(B)** Western blotting images of p-p65, (total) p65 and GAPDH in the liver, and quantifications of p-p65/(total) p65 ratio; **(C)** Western blotting images of p-ERK, (total) ERK and GAPDH in the liver, and quantifications of p-ERK/(total) ERK ratio; **(D)** Western blotting images of p-p38, (total) p38 and GAPDH in the liver, and quantifications of p-p38/(total) p38 ratio; **(E)** Western blotting images of p-JNK, (total) JNK and GAPDH in the liver, and quantifications of p-JNK/(total) JNK ratio; n = 3 mice in each group. Results are expressed as means ± SD. *p < 0.05, **p < 0.01, ***p < 0.001, ****p < 0.0001.

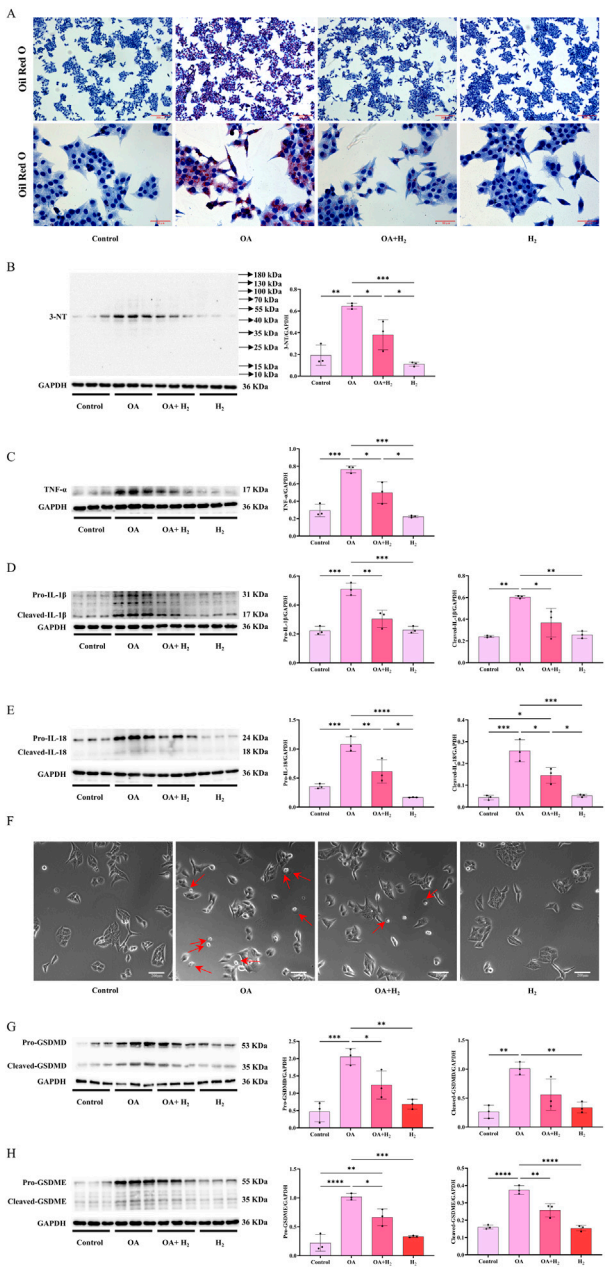

FIGURE 9
H_2-rich medium improved OA-induced steatosis in HepG2 cells by inhibiting inflammatory cytokines expression and pyroptosis. **(A)** The Oil Red O staining of HepG2 cells. **(B)** Western blotting images of 3-NT and GAPDH in HepG2 cells, and quantifications of 3-NT/GAPDH ratio. **(C)** Western blotting images of TNFα and GAPDH in HepG2 cells, and quantifications of TNFα/GAPDH ratio. **(D)** Western blotting images of IL-1β and GAPDH in HepG2 cells, and quantifications of pro-IL-1β/GAPDH and cleaved-IL-1β/GAPDH ratios. **(E)** Western blotting images of IL-18 and GAPDH in HepG2 cells, and quantifications of pro-IL-18/GAPDH and cleaved-IL-18/GAPDH ratios. **(F)** The images of pyroptosis morphology of HepG2 cells observed under the bright field. **(G)** Western blotting images of pro-GSDMD, cleaved-GSDMD and GAPDH in the liver, and quantifications of pro-GSDMD/GAPDH and cleaved-GSDMD/GAPDH ratios. **(H)** Western blotting images of pro-GSDME, cleaved-GSDME and GAPDH in HepG2 cells, and quantifications of pro-GSDME/GAPDH and cleaved-GSDME/GAPDH ratios. Results are expressed as means ± SD. *p < 0.05, **p < 0.01, ***p < 0.001, ****p < 0.0001.

MDA increased, and the antioxidant GSH in the liver of mice fed with a MCD diet decreased, these indicated that MCD diet feeding disturbed hepatic redox homeostasis, which was improved by H_2 treatment. It is known that H_2 selectively reduced the hydroxyl radical, the most cytotoxic of ROS, and effectively protected cells (Ohsawa et al., 2007). H_2 can also reduce the expression of NADPH oxidase subunit p67 (phox) expression (Zhang et al., 2016). However, the detail mechanism by which H_2 improves redox homeostasis in MASLD still requires further exploration.

Pyroptosis is a key mechanism of MASLD (Xu et al., 2018; Gaul et al., 2021). Pyroptosis is executed by the pore-forming protein GSDMD, which is always activated/cleaved by Caspase-1, murine Caspase-11 and its human orthologs Caspase-4 and Caspase-5, and Caspase-8 (Shi et al., 2017; Orning et al., 2018; Sarhan et al., 2018; Rathinam et al., 2019). The activated canonical inflammasomes, such as NLRP3 inflammasome, by the ligands can activate Caspase-1; Caspase-4, Caspase-5, and Caspase-11 can directly recognize bacterial LPS; both of which trigger pyroptosis by cleaved GSDMD (Shi et al., 2015). NLRP3 inflammasome includes three major components: NLRP3, Caspase-1, and ASC (apoptosis-associated speck-like protein containing a caspase recruitment domain), which acts as a bridge connecting NLRP3 and Caspase-1 (Fu and Wu, 2023). The protein levels of NLRP3, ASC, full-length and the cleaved forms of Caspase-1 and GSDMD in the liver were increased by feeding a MCD diet, and these upregulation were decreased by intraperitoneal injection of H_2. These indicated that H_2 can inhibit NLRP3 inflammasome-mediated canonical pyroptosis signaling in the liver of MASLD mice. This canonical pyroptosis signaling was also inhibited by H_2 inhalation in myocardial infarction rat model and in myocardial I/R injury rat model (Nie et al., 2021a; Nie et al., 2021b). The non-canonical pyroptosis signaling, such as Caspase-11 and Caspase-8 to cleave GSDMD, and Caspase-3 to cleave GSDME (Kayagaki et al., 2015; Wang et al., 2017; Sarhan et al., 2018), were increased in the liver of mice fed with a MCD diet. These non-canonical pyroptosis signaling were suppressed by H_2 therapy. Recently, our group also showed that intraperitoneal injection of H_2 can alleviate acute ethanol-induced hepatotoxicity in mice partially via inhibiting Caspase-11 and Caspase-8 to GSDMD, and Caspase-3 to GSDME non-canonical pyroptosis signaling in the liver (Xu et al., 2024). These indicate that H_2 is an anti-pyroptosis gas molecule, and this is one of the key mechanisms of H_2 on treating MASLD in mice (Figure 10).

In addition to cleaving GSDMD to trigger pyroptosis, the cleaved Caspase-1 can also induced the cleavage of IL-1β and IL-18, and GSDMD is not only an executor of pyroptosis, but is also required for IL-1β secretion (He et al., 2015; Shi et al., 2015). As mentioned above, inflammation is also one of the key pathogeneses of MASLD. MCD diet feeding increased hepatic levels of TNF-α, the full length and cleaved forms of IL-1β and IL-18, and these can be suppressed by H_2. Like this, H_2 also showed the anti-inflammation effect in the heart, brain, kidney, and the sex organs (Zhang et al., 2018; Zhang et al., 2020a; Zhang et al., 2021b). We, therefore, investigated the mechanism of downregulation of inflammatory cytokines by H_2. It has been reported that LPS, which can be

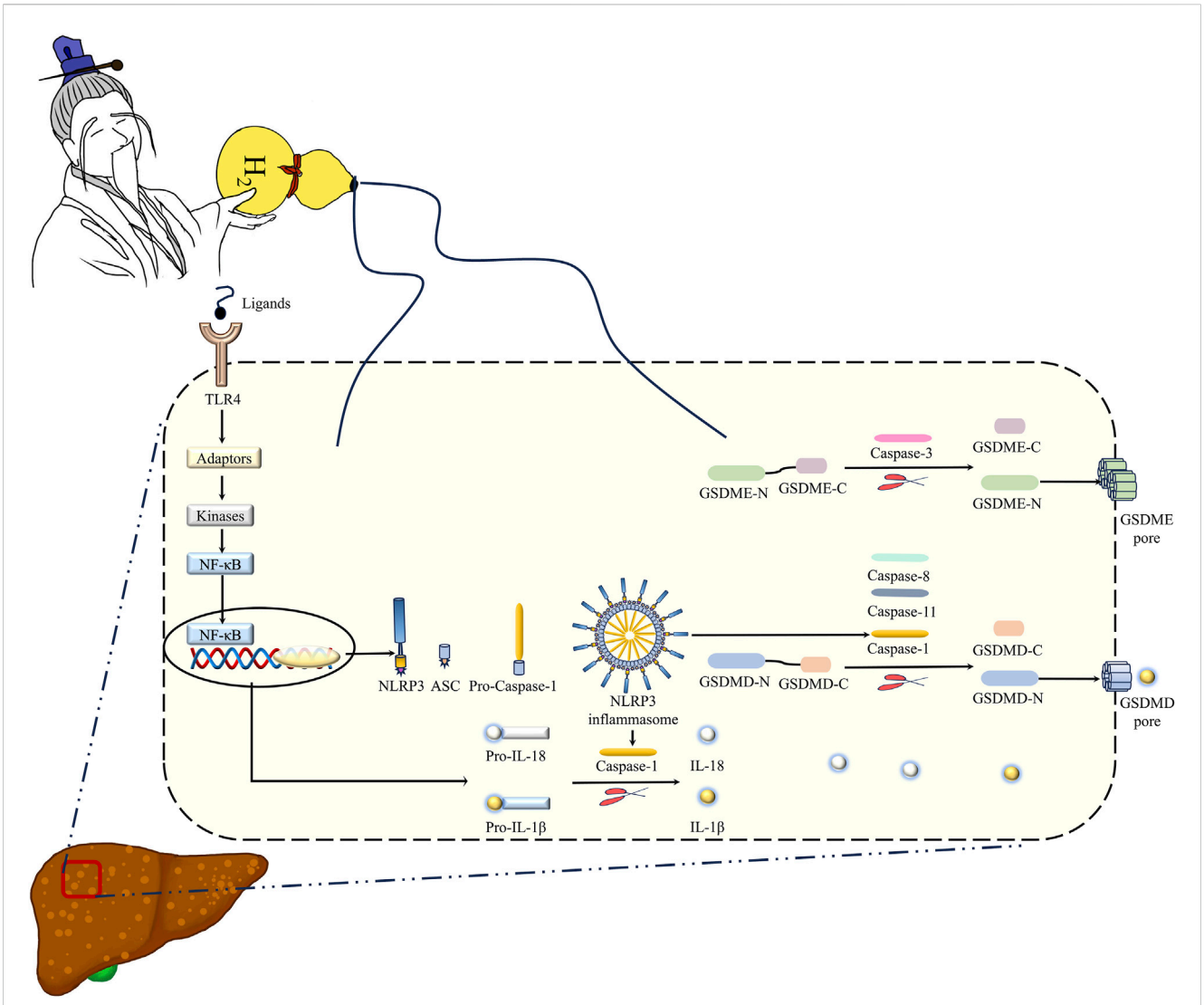

FIGURE 10
Hydrogen gas (H_2) is the immortal energy that subdues demons and monsters. H_2 is like the immortal qi in the treasure gourd of the immortal grandfather in Chinese mythology, which can subdue demons and eliminate evil spirits. Intraperitoneal injection of H_2, as a novel method for H_2 delivery, can alleviate MCD diet-induced MASLD in mice via inhibiting hepatic oxidative stress, TLR4-mediated innate immune signaling, and GSDMD- and GSDME-mediated pyroptosis. Therefore, H_2 therapy may act as a novel therapeutic strategy for MASLD in animals, which is worth further investigation.

recognized by the PRRs such as TLR4, was increased in MASLD mice model and patients (Carpino et al., 2020). TLR4 can elicit IKK phosphorylation to induce NF-κB-mediated inflammatory cytokines expression, or elicit MAPK (ERK1/2, p38 MAPK and JNK) phosphorylation to induce AP-1-mediated inflammatory cytokines expression (Zhang et al., 2017a; Zhang and Li, 2017; Zhang et al., 2017b). The expression of TLR4, the phosphorylation of NF-κB, ERK1/2, p38 MAPK and JNK were increased in the liver of mice fed with a MCD diet. H_2 can reverse the overactivation of TLR4-mediated innate immune signaling in the liver (Figure 10). Our previously study also showed that the activation of NF-κB and MAPK signaling were suppressed by H_2 in animal models of alcoholic liver disease and septic cardiomyopathy. However, it is unclear whether H_2 can directly inhibits the phosphorylation of these molecules or suppressed their upstream molecules, or indirectly activates the negative molecules of innate immunity.

Data availability statement

The original contributions presented in the study are included in the article/supplementary material, further inquiries can be directed to the corresponding authors.

Ethics statement

The animal study was approved by Institutional Animal Care and Use Committee of Guangzhou University of Chinese Medicine

(Approval No. 2023053006). The study was conducted in accordance with the local legislation and institutional requirements.

Author contributions

YC: Writing – original draft, Investigation, Methodology. KW: Investigation, Writing – review and editing. WG: Investigation, Writing – review and editing. CL: Investigation, Data curation, Writing – review and editing. WS: Formal Analysis, Writing – original draft. QL: Investigation, Resources, Writing – review and editing. YD: Investigation, Data curation, Formal Analysis, Writing – review and editing. XC: Formal Analysis, Investigation, Writing – review and editing. MD: Funding acquisition, Supervision, Writing – review and editing. XZ: Investigation, Project administration, Writing – review and editing. JX: Supervision, Writing – review and editing. WS: Investigation, Project administration, Writing – review and editing. SY: Project administration, Supervision, Writing – review and editing. HY: Supervision, Writing – review and editing. FY: Supervision, Writing – review and editing. HL: Supervision, Writing – review and editing. YZ: Supervision, Conceptualization, Funding acquisition, Writing – original draft, Writing – review and editing.

Funding

The author(s) declare that financial support was received for the research and/or publication of this article. This research was funded by Medical Research Foundation of Guangdong Province (B2025183), Research Project of Guangdong Provincial Bureau of Traditional Chinese Medicine (TCM) (20231103, 20241081, and 20241055), Flagship Department Construction Project for Collaborative TCM and Western Medicine (The comprehensive letter of TCM [2024] NO. 221, 2025TGL0370000014), Natural Science Foundation of Guangdong Province (2023A1515012828), Special Project for Key Fields of Guangdong Provincial Ordinary Colleges and Universities (2024ZDZX2042), National Natural Science Foundation of China (81900376), Construction Project of Inheritance Studio of National Famous and Old TCM Expert Yang Hongzhi (140000020162), and Guangdong Province Key Discipline Construction Project of TCM (20220104).

Conflict of interest

The authors declare that the research was conducted in the absence of any commercial or financial relationships that could be construed as a potential conflict of interest.

Generative AI statement

The author(s) declare that no Generative AI was used in the creation of this manuscript.

Publisher's note

References

Amini-Salehi, E., Letafatkar, N., Norouzi, N., Joukar, F., Habibi, A., Javid, M., et al. (2024). Global prevalence of nonalcoholic fatty liver disease: an updated review meta-analysis comprising a population of 78 million from 38 countries. *Archives Med. Res.* 55 (6), 103043. doi:10.1016/j.arcmed.2024.103043

Ayala, A., Muñoz, M. F., and Argüelles, S. (2014). Lipid peroxidation: production, metabolism, and signaling mechanisms of malondialdehyde and 4-hydroxy-2-nonenal. *Oxid. Med. Cell Longev.* 2014, 360438. doi:10.1155/2014/360438

Carpino, G., Del Ben, M., Pastori, D., Carnevale, R., Baratta, F., Overi, D., et al. (2020). Increased liver localization of lipopolysaccharides in human and experimental NAFLD. *Hepatology* 72 (2), 470–485. doi:10.1002/hep.31056

Chalasani, N., Younossi, Z., Lavine, J. E., Charlton, M., Cusi, K., Rinella, M., et al. (2017). The diagnosis and management of nonalcoholic fatty liver disease: practice guidance from the American association for the study of liver diseases. *Hepatology* 67 (1), 328–357. doi:10.1002/hep.29367

Chen, C., Ma, Y., Gong, W., Zhang, H., Wang, J., Yang, Z., et al. (2020). Steatosis and inflammation of L02 hepatocytes induced by sodium oleate. *Wei Sheng Yan Jiu* 49 (3), 381–385. doi:10.19813/j.cnki.weishengyanjiu

Chen, Z., Liu, J., Zhou, F., Li, H., Zhang, X. J., She, Z. G., et al. (2021). Nonalcoholic fatty liver disease: an emerging driver of cardiac arrhythmia. *Circ. Res.* 128 (11), 1747–1765. doi:10.1161/circresaha.121.319059

Day, C. P., and James, O. F. (1998). Steatohepatitis: a tale of two hits. *Gastroenterology* 114 (4), 842–845. doi:10.1016/s0016-5085(98)70599-2

Ding, J., Wang, K., Liu, W., She, Y., Sun, Q., Shi, J., et al. (2016). Pore-forming activity and structural autoinhibition of the gasdermin family. *Nature* 535 (7610), 111–116. doi:10.1038/nature18590

Fu, J., and Wu, H. (2023). Structural mechanisms of NLRP3 inflammasome assembly and activation. *Annu. Rev. Immunol.* 41, 301–316. doi:10.1146/annurev-immunol-081022-021207

Gaul, S., Leszczynska, A., Alegre, F., Kaufmann, B., Johnson, C. D., Adams, L. A., et al. (2021). Hepatocyte pyroptosis and release of inflammasome particles induce stellate cell activation and liver fibrosis. *J. Hepatol.* 74 (1), 156–167. doi:10.1016/j.jhep.2020.07.041

Ge, Y. S., Zhang, Q. Z., Li, H., Bai, G., Jiao, Z. H., and Wang, H. B. (2019). Hydrogen-rich saline protects against hepatic injury induced by ischemia-reperfusion and laparoscopic hepatectomy in swine. *Hepatobiliary Pancreat. Dis. Int.* 18 (1), 48–61. doi:10.1016/j.hbpd.2018.12.001

Gyamfi, M. A., Damjanov, I., French, S., and Wan, Y. J. (2008). The pathogenesis of ethanol versus methionine and choline deficient diet-induced liver injury. *Biochem. Pharmacol.* 75 (4), 981–995. doi:10.1016/j.bcp.2007.09.030

Hagström, H., Vessby, J., Ekstedt, M., and Shang, Y. (2024). 99% of patients with NAFLD meet MASLD criteria and natural history is therefore identical. *J. Hepatol.* 80 (2), e76–e77. doi:10.1016/j.jhep.2023.08.026

Hatting, M., Zhao, G., Schumacher, F., Sellge, G., Al Masaoudi, M., Gaßler, N., et al. (2013). Hepatocyte caspase-8 is an essential modulator of steatohepatitis in rodents. *Hepatology* 57 (6), 2189–2201. doi:10.1002/hep.26271

He, W.-T., Wan, H., Hu, L., Chen, P., Wang, X., Huang, Z., et al. (2015). Gasdermin D is an executor of pyroptosis and required for interleukin-1β secretion. *Cell Res.* 25 (12), 1285–1298. doi:10.1038/cr.2015.139

Henao-Mejia, J., Elinav, E., Jin, C., Hao, L., Mehal, W. Z., Strowig, T., et al. (2012). Inflammasome-mediated dysbiosis regulates progression of NAFLD and obesity. *Nature* 482 (7384), 179–185. doi:10.1038/nature10809

Hu, Z., Yue, H., Jiang, N., and Qiao, L. (2025). Diet, oxidative stress and MAFLD: a mini review. *Front. Nutr.* 12, 1539578. doi:10.3389/fnut.2025.1539578

Huang, G., Zhou, J., Zhan, W., Xiong, Y., Hu, C., Li, X., et al. (2013). The neuroprotective effects of intraperitoneal injection of hydrogen in rabbits with cardiac arrest. *Resuscitation* 84 (5), 690–695. doi:10.1016/j.resuscitation.2012.10.018

Ipsen, D. H., Lykkesfeldt, J., and Tveden-Nyborg, P. (2018). Molecular mechanisms of hepatic lipid accumulation in non-alcoholic fatty liver disease. *Cell Mol. Life Sci.* 75 (18), 3313–3327. doi:10.1007/s00018-018-2860-6

Kayagaki, N., Stowe, I. B., Lee, B. L., O'Rourke, K., Anderson, K., Warming, S., et al. (2015). Caspase-11 cleaves gasdermin D for non-canonical inflammasome signalling. *Nature* 526 (7575), 666–671. doi:10.1038/nature15541

Keam, S. J. (2024). Resmetirom: first approval. *Drugs* 84 (6), 729–735. doi:10.1007/s40265-024-02045-0

Kirsch, R., Clarkson, V., Shephard, E. G., Marais, D. A., Jaffer, M. A., Woodburne, V. E., et al. (2003). Rodent nutritional model of non-alcoholic steatohepatitis: species, strain and sex difference studies. *J. Gastroenterol. Hepatol.* 18 (11), 1272–1282. doi:10.1046/j.1440-1746.2003.03198.x

Kleiner, D. E., Brunt, E. M., Van Natta, M., Behling, C., Contos, M. J., Cummings, O. W., et al. (2005). Design and validation of a histological scoring system for nonalcoholic fatty liver disease. *Hepatology* 41 (6), 1313–1321. doi:10.1002/hep.20701

Li, Y., Yang, P., Ye, J., Xu, Q., Wu, J., and Wang, Y. (2024). Updated mechanisms of MASLD pathogenesis. *Lipids Health Dis.* 23 (1), 117. doi:10.1186/s12944-024-02108-x

Liang, B., Shi, L., Du, D., Li, H., Yi, N., Xi, Y., et al. (2023). Hydrogen-rich water ameliorates metabolic disorder via modifying gut microbiota in impaired fasting glucose patients: a randomized controlled study. *Antioxidants (Basel)* 12 (6), 1245. doi:10.3390/antiox12061245

Liang, W., Menke, A. L., Driessen, A., Koek, G. H., Lindeman, J. H., Stoop, R., et al. (2014). Establishment of a general NAFLD scoring system for rodent models and comparison to human liver pathology. *PLoS One* 9 (12), e115922. doi:10.1371/journal.pone.0115922

Liu, D., Zhang, P., Zhou, J., Liao, R., Che, Y., Gao, M. M., et al. (2020). TNFAIP3 interacting protein 3 overexpression suppresses nonalcoholic steatohepatitis by blocking TAK1 activation. *Cell Metab.* 31 (4), 726–740. doi:10.1016/j.cmet.2020.03.007

Liu, H., Kang, X., Ren, P., Kuang, X., Yang, X., Yang, H., et al. (2023). Hydrogen gas ameliorates acute alcoholic liver injury via anti-inflammatory and antioxidant effects and regulation of intestinal microbiota. *Int. Immunopharmacol.* 120, 110252. doi:10.1016/j.intimp.2023.110252

Machado, M. V., Michelotti, G. A., Xie, G., Almeida Pereira, T., Boursier, J., Bohnic, B., et al. (2015). Mouse models of diet-induced nonalcoholic steatohepatitis reproduce the heterogeneity of the human disease. *PLoS One* 10 (5), e0127991. doi:10.1371/journal.pone.0127991

Mackowiak, B., Xu, M., Lin, Y., Guan, Y., Seo, W., Ren, R., et al. (2022). Hepatic CYP2B10 is highly induced by binge ethanol and contributes to acute-on-chronic alcohol-induced liver injury. *Alcohol Clin. Exp. Res.* 46 (12), 2163–2176. doi:10.1111/acer.14954

Mallet, M., Silaghi, C. A., Sultanik, P., Conti, F., Rudler, M., Ratziu, V., et al. (2024). Current challenges and future perspectives in treating patients with NAFLD-Related cirrhosis. *Hepatology* 80 (5), 1270–1290. doi:10.1097/hep.0000000000000456

Mehlem, A., Hagberg, C. E., Muhl, L., Eriksson, U., and Falkevall, A. (2013). Imaging of neutral lipids by oil red O for analyzing the metabolic status in health and disease. *Nat. Protoc.* 8 (6), 1149–1154. doi:10.1038/nprot.2013.055

Miao, L., Targher, G., Byrne, C. D., Cao, Y. Y., and Zheng, M. H. (2024). Current status and future trends of the global burden of MASLD. *Trends Endocrinol. Metab.* 35 (8), 697–707. doi:10.1016/j.tem.2024.02.007

Nie, C., Ding, X., A, R., Zheng, M., Li, Z., Pan, S., et al. (2021a). Hydrogen gas inhalation alleviates myocardial ischemia-reperfusion injury by the inhibition of oxidative stress and NLRP3-mediated pyroptosis in rats. *Life Sci.* 272, 119248. doi:10.1016/j.lfs.2021.119248

Nie, C., Zou, R., Pan, S., A, R., Gao, Y., Yang, H., et al. (2021b). Hydrogen gas inhalation ameliorates cardiac remodelling and fibrosis by regulating NLRP3 inflammasome in myocardial infarction rats. *J. Cell Mol. Med.* 25 (18), 8997–9010. doi:10.1111/jcmm.16863

Ohsawa, I., Ishikawa, M., Takahashi, K., Watanabe, M., Nishimaki, K., Yamagata, K., et al. (2007). Hydrogen acts as a therapeutic antioxidant by selectively reducing cytotoxic oxygen radicals. *Nat. Med.* 13 (6), 688–694. doi:10.1038/nm1577

Orning, P., Weng, D., Starheim, K., Ratner, D., Best, Z., Lee, B., et al. (2018). Pathogen blockade of TAK1 triggers caspase-8-dependent cleavage of gasdermin D and cell death. *Science* 362 (6418), 1064–1069. doi:10.1126/science.aau2818

Pickens, M. K., Yan, J. S., Ng, R. K., Ogata, H., Grenert, J. P., Beysen, C., et al. (2009). Dietary sucrose is essential to the development of liver injury in the methionine-choline-deficient model of steatohepatitis. *J. Lipid Res.* 50 (10), 2072–2082. doi:10.1194/jlr.M900022-JLR200

Pierce, A. A., Pickens, M. K., Siao, K., Grenert, J. P., and Maher, J. J. (2015). Differential hepatotoxicity of dietary and DNL-Derived palmitate in the methionine-choline-deficient model of steatohepatitis. *BMC Gastroenterol.* 15, 72. doi:10.1186/s12876-015-0298-y

Rathinam, V. A. K., Zhao, Y., and Shao, F. (2019). Innate immunity to intracellular LPS. *Nat. Immunol.* 20 (5), 527–533. doi:10.1038/s41590-019-0368-3

Rinella, M. E., Elias, M. S., Smolak, R. R., Fu, T., Borensztajn, J., and Green, R. M. (2008). Mechanisms of hepatic steatosis in mice fed a lipogenic methionine choline-deficient diet. *J. Lipid Res.* 49 (5), 1068–1076. doi:10.1194/jlr.M800042-JLR200

Rinella, M. E., Lazarus, J. V., Ratziu, V., Francque, S. M., Sanyal, A. J., Kanwal, F., et al. (2023). A multisociety Delphi consensus statement on new fatty liver disease nomenclature. *J. Hepatol.* 79 (6), 1542–1556. doi:10.1016/j.jhep.2023.06.003

Rizki, G., Arnaboldi, L., Gabrielli, B., Yan, J., Lee, G. S., Ng, R. K., et al. (2006). Mice fed a lipogenic methionine-choline-deficient diet develop hypermetabolism coincident with hepatic suppression of SCD-1. *J. Lipid Res.* 47 (10), 2280–2290. doi:10.1194/jlr.M600198-JLR200

Sarhan, J., Liu, B. C., Muendlein, H. I., Li, P., Nilson, R., Tang, A. Y., et al. (2018). Caspase-8 induces cleavage of gasdermin D to elicit pyroptosis during yersinia infection. *Proc. Natl. Acad. Sci.* 115 (46), e10888–e10897. doi:10.1073/pnas.1809548115

Sarkar, M., and Kushner, T. (2025). Metabolic dysfunction-associated steatotic liver disease and pregnancy. *J. Clin. Invest* 135 (10), e186426. doi:10.1172/jci186426

Shi, J., Gao, W., and Shao, F. (2017). Pyroptosis: gasdermin-mediated programmed necrotic cell death. *Trends Biochem. Sci.* 42 (4), 245–254. doi:10.1016/j.tibs.2016.10.004

Shi, J., Zhao, Y., Wang, K., Shi, X., Wang, Y., Huang, H., et al. (2015). Cleavage of GSDMD by inflammatory caspases determines pyroptotic cell death. *Nature* 526 (7575), 660–665. doi:10.1038/nature15514

Sinha, R. A., Bruinstroop, E., and Yen, P. M. (2024). Actions of thyroid hormones and thyromimetics on the liver. *Nat. Rev. Gastroenterol. Hepatol.* 22, 9–22. doi:10.1038/s41575-024-00991-4

Sun, H., Chen, L., Zhou, W., Hu, L., Li, L., Tu, Q., et al. (2011). The protective role of hydrogen-rich saline in experimental liver injury in mice. *J. Hepatol.* 54 (3), 471–480. doi:10.1016/j.jhep.2010.08.011

Tan, S., Long, Z., Hou, X., Lin, Y., Xu, J., You, X., et al. (2019). H2 protects against lipopolysaccharide-induced cardiac dysfunction *via* blocking TLR4-Mediated cytokines expression. *Front. Pharmacol.* 10, 865. doi:10.3389/fphar.2019.00865

Targher, G., Byrne, C. D., and Tilg, H. (2024). MASLD: a systemic metabolic disorder with cardiovascular and malignant complications. *Gut* 73 (4), 691–702. doi:10.1136/gutjnl-2023-330595

Tilg, H., and Moschen, A. R. (2010). Evolution of inflammation in nonalcoholic fatty liver disease: the multiple parallel hits hypothesis. *Hepatology* 52 (5), 1836–1846. doi:10.1002/hep.24001

Valdecantos, M. P., Pardo, V., Ruiz, L., Castro-Sánchez, L., Lanzón, B., Fernández-Millán, E., et al. (2017). A novel glucagon-like peptide 1/glucagon receptor dual agonist improves steatohepatitis and liver regeneration in mice. *Hepatology* 65 (3), 950–968. doi:10.1002/hep.28962

Wang, Y., Gao, W., Shi, X., Ding, J., Liu, W., He, H., et al. (2017). Chemotherapy drugs induce pyroptosis through caspase-3 cleavage of a gasdermin. *Nature* 547 (7661), 99–103. doi:10.1038/nature22393

Wang, Y., Wang, Y., Li, F., Zou, J., Li, X., Xu, M., et al. (2022). Psoralen suppresses lipid deposition by alleviating insulin resistance and promoting autophagy in oleate-induced L02 cells. *Cells* 11 (7), 1067. doi:10.3390/cells11071067

Wrotek, S., Sobocińska, J., Kozłowski, H. M., Pawlikowska, M., Jędrzejewski, T., and Dzialuk, A. (2020). New insights into the role of glutathione in the mechanism of fever. *Int. J. Mol. Sci.* 21 (4), 1393. doi:10.3390/ijms21041393

Wu, C. W., Chu, E. S., Lam, C. N., Cheng, A. S., Lee, C. W., Wong, V. W., et al. (2010). PPARgamma is essential for protection against nonalcoholic steatohepatitis. *Gene Ther.* 17 (6), 790–798. doi:10.1038/gt.2010.41

Xu, B., Jiang, M., Chu, Y., Wang, W., Chen, D., Li, X., et al. (2018). Gasdermin D plays a key role as a pyroptosis executor of non-alcoholic steatohepatitis in humans and mice. *J. Hepatol.* 68 (4), 773–782. doi:10.1016/j.jhep.2017.11.040

Xu, L., Guo, W., Dai, J., Cheng, Y., Chen, Y., Liu, W., et al. (2024). Hydrogen gas alleviates acute ethanol-induced hepatotoxicity in mice via modulating TLR4/9 innate immune signaling and pyroptosis. *Int. Immunopharmacol.* 127, 111399. doi:10.1016/j.intimp.2023.111399

Younossi, Z. M., Zelber-Sagi, S., Henry, L., and Gerber, L. H. (2023). Lifestyle interventions in nonalcoholic fatty liver disease. *Nat. Rev. Gastroenterol. Hepatol.* 20 (11), 708–722. doi:10.1038/s41575-023-00800-4

Yu, Y., Liu, Y., An, W., Song, J., Zhang, Y., and Zhao, X. (2019). STING-Mediated inflammation in kupffer cells contributes to progression of nonalcoholic steatohepatitis. *J. Clin. Invest* 129 (2), 546–555. doi:10.1172/jci121842

Zhai, X., Chen, X., Lu, J., Zhang, Y., Sun, X., Huang, Q., et al. (2017). Hydrogen-rich saline improves non-alcoholic fatty liver disease by alleviating oxidative stress and activating hepatic PPARα and PPARγ. *Mol. Med. Rep.* 15 (3), 1305–1312. doi:10.3892/mmr.2017.6120

Zhang, Y., Bi, M., Chen, Z., Dai, M., Zhou, G., Hu, Y., et al. (2021a). Hydrogen gas alleviates acute alcohol-induced liver injury by inhibiting JNK activation. *Exp. Ther. Med.* 21 (5), 453. doi:10.3892/etm.2021.9884

Zhang, Y., Huang, Z., and Li, H. (2017a). Insights into innate immune signalling in controlling cardiac remodelling. *Cardiovasc Res.* 113 (13), 1538–1550. doi:10.1093/cvr/cvx130

Zhang, Y., and Li, H. (2017). Reprogramming interferon regulatory factor signaling in cardiometabolic diseases. *Physiol. (Bethesda)* 32 (3), 210–223. doi:10.1152/physiol.00038.2016

Zhang, Y., Liu, H., Xu, J., Zheng, S., and Zhou, L. (2021b). Hydrogen gas: a novel type of antioxidant in modulating sexual organs homeostasis. *Oxid. Med. Cell Longev.* 2021, 8844346. doi:10.1155/2021/8844346

Zhang, Y., Tan, S., Xu, J., and Wang, T. (2018). Hydrogen therapy in cardiovascular and metabolic diseases: from bench to bedside. *Cell Physiol. Biochem.* 47 (1), 1–10. doi:10.1159/000489737

Zhang, Y., Xu, J., Long, Z., Wang, C., Wang, L., Sun, P., et al. (2016). Hydrogen (H(2)) inhibits isoproterenol-induced cardiac hypertrophy via antioxidative pathways. *Front. Pharmacol.* 7, 392. doi:10.3389/fphar.2016.00392

Zhang, Y., Xu, J., and Yang, H. (2020a). Hydrogen: an endogenous regulator of liver homeostasis. *Front. Pharmacol.* 11, 877. doi:10.3389/fphar.2020.00877

Zhang, Y., Zhang, J., Xu, K., Chen, Z., Xu, X., Xu, J., et al. (2020b). Helium protects against lipopolysaccharide-induced cardiac dysfunction in mice *via* suppressing toll-like receptor 4-Nuclear factor κB-Tumor necrosis Factor-Alpha/Interleukin-18 signaling. *Chin. J. Physiol.* 63 (6), 276–285. doi:10.4103/cjp.Cjp_66_20

Zhang, Y., Zhang, X. J., Wang, P. X., Zhang, P., and Li, H. (2017b). Reprogramming innate immune signaling in cardiometabolic disease. *Hypertension* 69 (5), 747–760. doi:10.1161/hypertensionaha.116.08192

Zhang, Y., Zhou, G., Chen, Z., Guan, W., Zhang, J., Bi, M., et al. (2020c). Si-wu-tang alleviates nonalcoholic fatty liver disease via blocking TLR4-JNK and Caspase-8-GSDMD signaling pathways. *Evid. Based Complement. Altern. Med.* 2020, 8786424. doi:10.1155/2020/8786424